ISSN 1674-1056
http://cpb.iphy.ac.cn
http://iopscience.iop.org/cpb
中国物理 B
Chinese Physics
中国物理 Chinese Physics B

Low drift nuclear spin gyroscope with probe light intensity error suppression

Wenfeng Fan(范文峰)[1], Wei Quan(全伟)[1,2,3], Feng Liu(刘峰)[1], Lihong Duan(段利红)[1], Gang Liu(刘刚)[1,2,3]
Citation: Chin. Phys. B . 2019, 28(11): 110701 . **doi:** 10.1088/1674-1056/ab44a5
Journal homepage: http://cpb.iphy.ac.cn; http://iopscience.iop.org/cpb

What follows is a list of articles you may be interested in

Miniature quad-channel spin-exchange relaxation-free magnetometer for magnetoencephalography

Jian-Jun Li(李建军), Peng-Cheng Du(杜鹏程), Ji-Qing Fu(伏吉庆), Xu-Tong Wang(王旭桐), Qing Zhou(周庆), Ru-Quan Wang(王如泉)
Chin. Phys. B . 2019, 28(4): 040703 . **doi:** 10.1088/1674-1056/28/4/040703

Observing the steady-state visual evoked potentials with a compact quad-channel spin exchange relaxation-free magnetometer

Peng-Cheng Du(杜鹏程), Jian-Jun Li(李建军), Si-Jia Yang(杨思嘉), Xu-Tong Wang(王旭桐), Yan Zhuo(卓彦), Fan Wang(王帆), Ru-Quan Wang(王如泉)
Chin. Phys. B . 2019, 28(4): 040702 . **doi:** 10.1088/1674-1056/28/4/040702

Magnetic field analysis in a diamond anvil cell for Meissner effect measurement by using the diamond NV^- center

Lin Zhao(赵琳), Donghui Yue(岳冬辉), Cailong Liu(刘才龙), Min Wang(王敏), Yonghao Han(韩永昊), Chunxiao Gao(高春晓)
Chin. Phys. B . 2019, 28(3): 030702 . **doi:** 10.1088/1674-1056/28/3/030702

Damage and recovery of fiber Bragg grating under radiation environment

Shi-Zhe Wen(温世喆), Wei-Chen Xiong(熊伟晨), Li-Ping Huang(黄力平), Zhen-Rui Wang(王镇锐), Xing-Bin Zhang(张兴斌), Zhen-Hui He(何振辉)
Chin. Phys. B . 2018, 27(9): 090701 . **doi:** 10.1088/1674-1056/27/9/090701

In-situ measurement of magnetic field gradient in a magnetic shield by a spin-exchange relaxation-free magnetometer

Fang Jian-Cheng, Wang Tao, Zhang Hong, Li Yang, Cai Hong-Wei
Chin. Phys. B . 2015, 24(6): 060702 . **doi:** 10.1088/1674-1056/24/6/060702

Low drift nuclear spin gyroscope with probe light intensity error suppression*

Wenfeng Fan(范文峰)[1,†], Wei Quan(全伟)[1,2,3], Feng Liu(刘峰)[1], Lihong Duan(段利红)[1], and Gang Liu(刘刚)[1,2,3]

[1] *School of Instrumentation and Optoelectronic Engineering, Beihang University, Beijing* 100191, *China*
[2] *Beijing Advanced Innovation Center for Big Data-Based Precision Medicine, Beihang University, Beijing* 100191, *China*
[3] *Beijing Academy of Quantum Information Sciences, Beijing* 100193, *China*

(Received 4 August 2019; published online 30 October 2019)

A nuclear spin gyroscope based on an alkali-metal–noble-gas co-magnetometer operated in spin-exchange relaxation-free (SERF) regime is a promising atomic rotation sensor for its ultra-high fundamental sensitivity. However, the fluctuation of probe light intensity is one of the main technical error sources that limits the bias stability of the gyroscope. Here we propose a novel method to suppress the bias error induced by probe light intensity fluctuations. This method is based on the inherent magnetic field response characteristics of the gyroscope. By the application of a bias magnetic field, the gyroscope can be tuned to a working point where the output signal is insensitive to probe light intensity variation, referred to herein as 'zero point', thus the bias error induced by intensity fluctuations can be completely suppressed. The superiority of the method was verified on a K–Rb–^{21}Ne co-magnetometer, and a bias stability of approximately 0.01 °/h was obtained. In addition, the method proposed here can remove the requirement of the closed-loop control of probe light intensity, thereby facilitating miniaturization of the gyroscope volume and improvement of reliability.

Keywords: nuclear spin gyroscope, spin-exchange relaxation-free, error suppression, probe light intensity

PACS: 07.07.Df, 07.55.Ge, 42.79.–e **DOI:** 10.1088/1674-1056/ab44a5

1. Introduction

High-precision gyroscopes have found wide applications in inertial navigation, geophysics studies, fundamental physics, and so on.[1,2] Among these applications, one of the factors determining system performance and experimental results is the bias stability of the gyroscope. While the accuracy of the traditional gyroscopes based on classical mechanics or Sagnac effect of photons has reached a high level,[3,4] the research on gyroscopes based on new mechanism is still in progress. As quantum sensing technology becomes a distinct field of research,[5] gyroscopes based on the fascinating property of ultrahigh sensitivity of atomic sensors have been developed, including atomic interferometer gyroscopes[6,7] and nuclear spin gyroscopes.[8,9] Nuclear spin gyroscopes have attracted a lot of research interest because of their high precision potential, easy integration, and insensitivity to vibration and gravity.[10] As the relaxation of coherent evolution qubits in a quantum system is a main factor that limits its performance, atomic magnetometers operated in spin-exchange relaxation-free (SERF) regime, where the relaxation of electron spins due to spin-exchange collisions is greatly suppressed, have become one of the most sensitive magnetometers to date.[11] Based on the ultrahigh magnetic sensitivity of SERF magnetometers, the Romalis group at Princeton University first proposed a novel type of nuclear spin gyroscope based on an alkali–metal–noble–gas co-magnetometer scheme in 2005, and a bias stability of 0.04 °/h was achieved on their K–^{3}He co-magnetometer.[12] This type of gyroscope is usually called spin-exchange relaxation-free gyroscope (SERFG) and it features ultrahigh rotation sensing sensitivity and magnetic field disturbance cancellation ability. After that, the principles and theories of the gyroscope have been intensively studied and verified. Our group demonstrated a dual-axis SERFG with parametrical modulation technique, and a bias stability of better than 0.05 °/h was achieved in 2018.[13] After that, it was found that magnetic field fluctuations can still cause bias drift in SERFG.[14] By the analysis of the magnetic field response of this gyroscope, the bias error induced by magnetic noise has been suppressed to 5×10^{-4} °/h.[15,16]

A SERFG usually utilizes an orthogonal pump-probe scheme.[17] A circularly polarized pump beam is used to pump the alkali–metal atoms, and a linearly polarized probe beam propagating along the direction perpendicular to the pump beam is used to detect the precession of atomic spin. The optical rotation of the probe beam is usually measured with a balanced photodetector[13] or polarization modulation technique.[18] As the scale factor of a SERFG is proportional to the light intensity of the probe beam, the light intensity fluctuations can couple into the output signal and induce bias

*Project supported by the National Key Research and Development Program of China (Grant Nos. 2016YFB0501600 and 2017YFB0503100) and the National Natural Science Foundation of China (Grant Nos. 61773043, 61673041, and 61721091).
†Corresponding author. E-mail: fanwenfeng@buaa.edu.cn
© 2019 Chinese Physical Society and IOP Publishing Ltd

drift. Therefore, light intensity stabilization system is usually used to suppress the fluctuations.[18] However, due to the temperature-dependent performance of optical components in the light intensity stabilization system (LISS), the intensity stabilization accuracy is greatly affected by the environment temperature variation.[19] In this letter, we propose a novel method to suppress the bias error induced by probe light intensity fluctuations. Based on the magnetic field response characteristic of SERFG,[15] a bias magnetic field is used to tune the system to the working point where the output signal is no longer sensitive to the probe light intensity variations. The superiority of our method was verified on a K–Rb–^{21}Ne comagnetometer, and a bias stability of approximately 0.01 °/h was achieved.

2. Theoretical method

The schematic diagram of a SERFG is similar to that in our previous literature,[16] and is depicted in Fig. 1. At the center of the gyroscope is a 10-mm-diameter spherical vapor cell with 760 Torr (1 Torr = 1.33322×10^2 Pa) of ^{21}Ne buffer gas, 50-Torr nitrogen quenching gas, and a mixture of K and Rb. The cell held in an oven made of non-magnetic ceramic material is heated to 185 °C by ac current-driven heating coils. And the density ratio between K and Rb is estimated to be 1 : 200. A tri-axial magnetic coil system is used for magnetic field compensation. The magnetic shielding system composed of two outer layers of μ-metal shields and one innermost ferrite shield is used to screen out the environmental magnetic field disturbance. Circularly polarized light tuned to 770.108 nm polarizes the K atoms. Rb atoms are polarized by K atoms through spin exchange. Linearly polarized light tuned to 795.38 nm is used to detect atomic spin precession and polarization modulation technique is used to measure the optical rotation angle. The intensity of lasers are controlled by an LISS.

A set of coupled Bloch equations are usually used to characterize the dynamics of the electron and nuclear spins in a SERFG. According to the theoretical and experimental results of the magnetic field transfer function analysis of SERFG,[15] the system can be described with a linear time-invariant system. When the polarization of atoms has reached equilibrium, an external compensation field $B_c = -B^n - B^e$ is employed along z axis to cancel the magnetic field from nuclear magnetization B^n and that from electron magnetization B^e. If we take the transverse rotation rate Ω_{xi} and Ω_{yi} , the transverse magnetic field B_{xi} and B_{yi} as system inputs, the leading steady state response terms of the gyroscope can be expressed as[18]

$$V_{\text{out}} = K_0 I_0 (\theta_c + \theta_r), \tag{1}$$

where K_0 is a constant factor and can be expressed as $K_0 = \eta G e^{-OD} \alpha_m$, in this expression, η is the photoelectric conversion efficiency, G is the gain of the preamplifier circuit of the LIA, OD is the optical depth, α_m is the modulation depth of the PEM. I_0 is incident probe light intensity, $\theta_c = K_1 P_x^e$ is the optical rotation angle caused by the atoms in the cell, K_1 is a constant factor independent of light intensity,[20] and P_x^e is the polarization of Rb atoms along x axis. θ_r is the unwanted optical rotation angle error caused by the imperfections of the cell and optical components. Keeping the leading terms of the gyroscope response, P_x^e can be expressed as

$$\begin{aligned} P_x^e = & \frac{P_z^e \gamma^e R_{\text{tot}}^e}{\left[(R_{\text{tot}}^e)^2 + (\delta B_z \gamma^e)^2\right](\delta B_z + B^n)} \\ & \times \left(\frac{B^n \Omega_{yi}}{\gamma^n} - \frac{R_{\text{tot}}^n}{\gamma^n} B_{xi} + \delta B_z^2 \frac{\gamma^e}{R_{\text{tot}}^e} \delta B_x \right. \\ & \left. + \delta B_z \delta B_y + \frac{\delta B_z \gamma^e}{R_{\text{tot}}^e} \frac{B^n \Omega_{xi}}{\gamma^n} \right). \end{aligned} \tag{2}$$

In order to distinguish from the input magnetic fields B_{xi} and B_{yi}, the deviation of the magnetic fields from compensation point $(0,0,B_c)$ are defined as δB_x, δB_y, and δB_z. P_z^e is the steady state polarization of electrons along z axis, γ^n is the gyromagnetic ratio of the nuclear-spin and γ^e is the gyromagnetic ratio of the electron-spin. R_{tot}^e is the transverse relaxation rate of electron-spin, R_{tot}^n is the transverse relaxation rate of nuclear-spin.

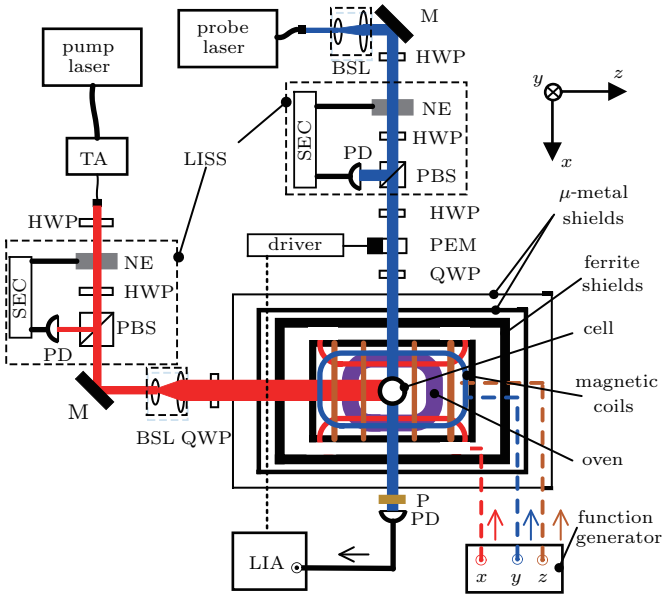


Fig. 1. Schematic diagram of the SERFG. TA: tapered amplifier, BSL: beam shaping lenses; M: reflection mirror; P: linear polarizer; NE: noise eater; HWP: half wave plate; PBS: polarizing beam splitter; QWP: quarter wave plate; PD: photodiode; PEM: photo-elastic modulator; LIA: lock-in amplifier; SEC: servo electronic circuit. An LISS mainly compromises of an NE, an HWP, a PBS, a PD, and an SEC. The output laser intensity of the LISS is monitored by the PD, which detects the intensity of a small portion of laser split by the PBS. The PD signal is fed into the SEC. The SEC compares the current laser intensity with the set-point value and changes the driving voltage applied to the NE to change the output laser intensity.

The compensation point is usually found based on Eq. (2). The δB_z can be zeroed by the application of a symmetric B_y modulation. According to the fourth term in the brackets,

when δB_z is exactly zero, the applied B_y modulation produces no signal difference in steady state. Once δB_z is zeroed, a similar symmetric B_z modulation around the point $\delta B_z = 0$ can be applied to zero δB_y. When the applied B_z modulation produces no steady state signal difference, the δB_y is zeroed.[14] As for the zeroing of δB_x, it is accomplished by modulating B_z asymmetrically between zero and a non-zero value. According to the third term in the brackets, the δB_x is zeroed when the asymmetrical modulation of B_z produces no steady state difference. When the magnetic fields are properly zeroed, the SERFG operates at the compensation point and its output signal can be obtained by substituting Eq. (2) into Eq. (1), which can be expressed as follows:

$$V_{\text{out}} = K_0 I_0 \left[K_1 \frac{P_z^{\text{e}} \gamma^{\text{e}}}{R_{\text{tot}}^{\text{e}}} \left(\frac{\Omega_{yi}}{\gamma^{\text{n}}} - \frac{R_{\text{tot}}^{\text{n}}}{B^{\text{n}} \gamma^{\text{n}}} B_{xi} \right) + \theta_{\text{r}} \right]. \tag{3}$$

It can be seen from Eq. (3) that at the compensation point, the gyroscope signal is proportional to I_0, meaning that intensity fluctuations will result in bias drift. Although an LISS is used to control the light intensity to the set-point, the actual I_0 will change with temperature as the split ratio of a PBS is temperature-dependent. The equivalent scale factor between light intensity and angular rate is measured and shown in Fig. 2 with the dash dotted line. Linear fitting of the experimental data gives a scale factor $K_{\Omega - I_0}$ of -104 °/h · mW^{-1}. When I_0 is nominally controlled by the LISS to 1.02 mW, its stability was experimentally evaluated and the drift of I_0 in 1 hour 9.8×10^{-5} mW in average, equivalent to a bias drift of 0.01 °/h. Fortunately, in addition to Ω_y, the output signal of the gyroscope is also proportional to B_x, and it can be accurately controlled by highly stable current source.

The basic idea of our method to suppress the error induced by probe light intensity fluctuations consists in employing a bias B_x field to tune the gyroscope to the working point where the steady state offset is zero, herein is called the 'zero point'. At zero point, the total optical rotation angle $(\theta_{\text{c}} + \theta_{\text{r}})$ in Eq. (1) is zero, so the equivalent scale factor of the probe light intensity is tuned to zero. Therefore, the variations of the probe light intensity will not affect the output of the gyroscope anymore. In the case of static test, the total offset of the gyroscope signal is mainly due to the earth's rotation Ω_{ye} and the residual rotation angle of the probe system. From Eq. (3), the zero point can be found when

$$\delta B_x = \delta B_{x0} = \frac{\gamma^{\text{n}} B^{\text{n}}}{R_{\text{tot}}^{\text{n}}} \left(\frac{\Omega_{ye}}{\gamma^{\text{n}}} + \frac{\theta_{\text{r}} R_{\text{tot}}^{\text{e}}}{K_1 P_z^{\text{e}} \gamma^{\text{e}}} \right). \tag{4}$$

3. Experimental results

As mentioned above, the equivalent scale factor of the probe light intensity can be tuned by B_x field, as is shown in Fig. 2. The scale factors were measured at different bias fields and a clear zero-crossing point can be found by the application of a probe light intensity modulation. In our experiment, the zero point is achieved when $B_x = -5.7$ nT. It should be noted that the existence of θ_{r} will cause additional bias field to reach zero point, resulting in the arise of spin-exchange relaxation rate.[11] Therefore, before polarizing the atoms, θ_{r} needs to be adjusted to zero as much as possible. Compared with the condition at compensation point, the drift induced by probe light intensity fluctuation can be completely eliminated theoretically. Our group have also demonstrated an SERFG based on Cs–^{129}Xe spin source with optical zeroing method to suppress the laser intensity fluctuation error.[21] Compared with the magnetic field zeroing method in this paper, the optical zeroing method requires the use of two Faraday modulators, which is not conducive to the miniaturization of the gyroscope. In addition, the optical error of the Faraday modulator itself cannot be completely eliminated. Therefore, from the perspective of future applications of an SERFG, magnetic field zeroing is more reasonable and effective. Question may arise that a gyroscope is used to measure the angular rate of its moving carrier, then the proposed method will fail in practical applications as the input angular rate is constantly changing. Considering that the measurement range of an SERFG is relatively small, a navigation scheme based on space-stable platform system is the optimal choice for it.[22] The platform system tracks an inertial coordinate system, so the angular rate input felt by the SERFG is constant. Therefore, from the perspective of future applications of an SERFG, the method is still feasible.

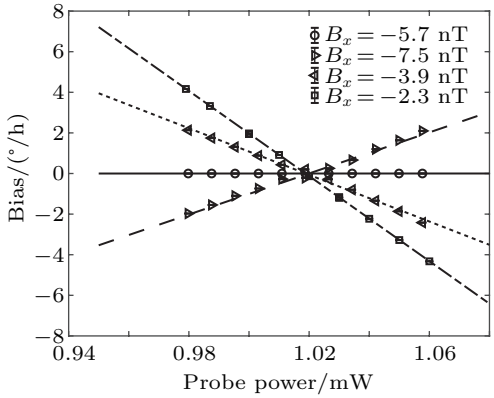


Fig. 2. Equivalent scale factor of the probe light intensity. The offset at $I_0 = 1.02$ mW is subtracted from all the signals. Dash dotted line with squares: $K_{\Omega - I_0} = -104$ °/h · mW^{-1} at $B_x = -2.3$ nT (compensation point); Solid line with circles: $K_{\Omega - I_0} = 0.03$ °/h · mW^{-1} at $B_x = -5.7$ nT (zero point); Dotted line with left triangles: $K_{\Omega - I_0} = -57.4$ °/h · mW^{-1} at $B_x = -3.9$ nT (positive offset); Dashed line with right triangles: $K_{\Omega - I_0} = 50.5$ °/h · mW^{-1} at $B_x = -7.5$ nT (negative offset). In our experiments, $K_{\Omega - I_0}$ at zero point can be suppressed by above three orders compared with that at compensation point. The error bars of the experimental data are plotted along with the lines, but they are too small to be distinguished.

To illustrate that our method does not introduce other errors, the scale factors and magnetic field sensitivities of the SERFG at compensation point and zero point were also compared. The scale factor are calibrated with low frequency modulation of B_x field[23] and the results are shown in Fig. 3. It can be seen that there is little difference between the scale factors and it is also verified with the calibration method on a rotatory platform.[13]

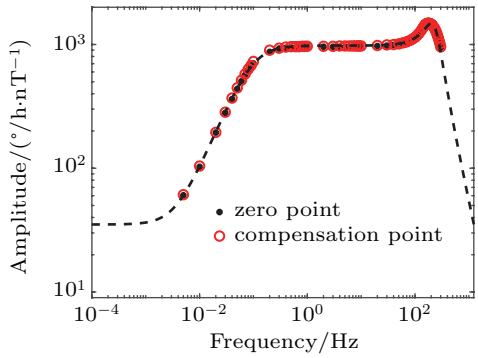


Fig. 3. Amplitude frequency response to B_x field. It can be seen that the amplitude responses of the SERFG at zero point and compensation point share the same fitting line,[15] meaning that the scale factors to angular rate are identical.

Another concern is the amplitudes of magnetic field response along three axes. When the gyroscope is working at zero point, the leading terms without steady state offset in Eq. (2) can be simplified as

$$P_x^{\mathrm{e}} = \frac{P_z^{\mathrm{e}}\gamma^{\mathrm{e}}}{R_{\mathrm{tot}}^{\mathrm{e}}}\left(\frac{\Omega_{yi}}{\gamma^{\mathrm{n}}} - \frac{R_{\mathrm{tot}}^{\mathrm{n}}}{\gamma^{\mathrm{n}}B^{\mathrm{n}}}B_{xi} + \delta B_z^2\frac{\gamma^{\mathrm{e}}}{B^{\mathrm{n}}R_{\mathrm{tot}}^{\mathrm{e}}}\delta B_{x0}\right). \quad (5)$$

The difference is that non-zero δB_{x0} introduces a δB_z^2 sensitive term. As is shown in Fig. 4, the dominant magnetic field sensitivity still comes from B_x. At zero point, the steady state response to δB_z is quadratic and there will be obvious deviations when $|\delta B_z| > 1$ nT. We experimentally measured that the magnetic field inside the shield drifts as small as 0.2 pT, so we can safely assume that δB_z will not introduce a dominant bias drift. And the equivalent drift cause by the drift of B_x is about 7×10^{-3} °/h.

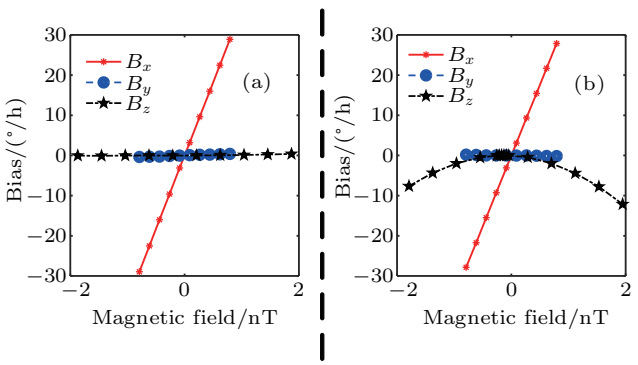


Fig. 4. Steady state response of the SERFG to magnetic fields along its three axes. The dominant magnetic field response comes from B_x, and linear fitting yields an equivalent scale factor of -33 °/h·nT^{-1}. The steady state offsets at both working points are subtracted from all the signals. (a) At compensation point and (b) at zero point.

The long term stability of the SERFG is evaluated by Allan deviation analysis and is shown in Fig. 5. The output signal is collected for a period of more than 5 hours with a sampling rate of 200 Hz while the gyroscope is kept stationary. The bias stability at the compensation point is about 0.02 °/h at an averaging time of 20 s, and the Allan deviation above 20 s is dominated by drift rate ramp induced by probe light intensity fluctuations. At the zero point, a bias stability of approximately 0.01 °/h at an averaging time of higher than 100 s is achieved. Therefore, the method proposed here can suppress the bias error caused by the fluctuations of probe light intensity and improve the long-term stability of the SERFG. And the dominant drift rate ramp above 1000 s may come from pump intensity fluctuations and the magnetic field drifts.

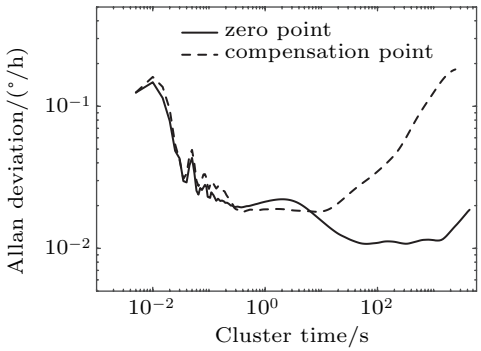


Fig. 5. Comparison of Allan deviation of the SERFG signal at static tests.

4. Conclusion

In conclusion, we have developed a low drift nuclear spin gyroscope based on a K–Rb–^{21}Ne co-magnetometer. Based on the magnetic field response characteristic, the working point of the gyroscope is tuned by B_x field from the compensation point to zero point where bias error induced by probe light intensity fluctuations can be completely suppressed, and no other errors are introduced. A bias stability of approximately 0.01 °/h is achieved. The method can remove the requirement of the closed-loop control of probe light intensity, thereby facilitating miniaturization of the gyroscope volume and improvement of reliability. In the future, we will devote to the suppression of the error induced by pump intensity fluctuations, to the suppression of magnetic field drift and to the closed-loop control of the zero point.

References

[1] Barbour N and Schmidt G 1998 *Proceedings of the 1998 Workshop on Autonomous Underwater Vehicles* (Cat. No. 98CH36290), August 21–21, 1998, Cambridge, MA, USA, p. 55
[2] Stedman G E 1997 *Rep. Prog. Phys.* **60** 615
[3] Greenspan R L 1995 *Navigation* **42** 165
[4] Lefevre H C 2013 *Opt. Fiber. Technol.* **19** 828

[5] Degen C L, Reinhard F and Cappellaro P 2017 *Rev. Mod. Phys.* **89** 035002
[6] Dickerson S M, Hogan J M, Sugarbaker A, Johnson D M and Kasevich M A 2013 *Phys. Rev. Lett.* **111** 083001
[7] Meng Z X, Li Y H and Feng Y Y 2018 *Chin. Phys. B* **27** 094201
[8] Meyer D and Larsen M 2014 *Gyroscopy and Navigation* **5** 75
[9] Zhang D W, Xu Z Y, Zhou M and Xu X Y 2017 *Chin. Phys. B* **26** 023201
[10] Zhang C, Yuan H, Tang Z, Quan W and Fang J C 2016 *Appl. Phys. Rev.* **3** 041305
[11] Allred J C, Lyman R N, Kornack T W and Romalis M V 2002 *Phys. Rev. Lett.* **89** 130801
[12] Kornack T W, Ghosh R K and Romalis M V 2005 *Phys. Rev. Lett.* **95** 230801
[13] Jiang L W, Quan W, Li R J, Fan W F, Liu F, Qin J, Wan S A and Fang J C 2018 *Appl. Phys. Lett.* **112** 054103
[14] Li R J, Quan W, Fan W F, Xing L and Fang J C 2017 *Sensors Actuat. A: Phys.* **266** 130
[15] Fan W F, Quan W, Zhang W J, Xing L and Liu G 2019 *IEEE Access* **7** 28574
[16] Fan W F, Quan W, Liu F, Xing L and Liu G 2019 *IEEE Sens. J.* **19** 9712
[17] Li R J, Fan W F, Jiang L W, Duan L H, Quan W and Fang J C 2016 *Phys. Rev. A* **94** 032109
[18] Duan L H, Fang J C, Li R J, Jiang L W, Ding M and Wang W 2015 *Opt. Express* **23** 32481
[19] Tricot F, Phung D H, Lours M, Guerandel S and de Clercq E 2018 *Rev. Sci. Instrum.* **89** 113112
[20] Ito S, Ito Y and Kobayashi T 2019 *Opt. Express* **27** 8037
[21] Fang J C, Wan S A, Qin J, Zhang C, Quan W, Yuan H, Dong H F and Fang J C 2013 *Rev. Sci. Instrum.* **84** 083108
[22] Cai Q Z, Yang G L, Quan W, Song N F, Tu Y Q and Liu Y L 2018 *Sensors* (Basel) **18** 670
[23] Brown J M, Smullin S J, Kornack T W and Romalis M V 2010 *Phys. Rev. Lett.* **105** 151604